INFRA-RED TUNNELING ABSORPTION IN SEMICONDUCTOR DOUBLE QUANTUM WELLS IN TILTED MAGNETIC FIELDS

S. K. LYO
Sandia National Laboratories, Albuquerque, N. M. 87185

ABSTRACT

Using a linear response theory, interwell-tunneling absorption is calculated in a double-quantum-well structure with a wide center barrier in tilted magnetic fields. Tunneling absorption of infra-red photons occurs between the ground sublevels of the two quantum wells, with an energy difference that is tunable. In zero magnetic field, the absorption intensity decreases significantly as the linewidth increases with temperature. The absorption also depends strongly on the carrier densities of the wells. In magnetic fields, both the in-plane and perpendicular components of the field sensitively control and tune the absorption lineshape in very different ways, affecting the absorption threshold, the resonance energy of absorption, and the linewidth.

INTRODUCTION

Long-wavelength infra-red (IR) detectors are currently receiving increasing attention for chemical sensing, thermal detection, and other applications. In this paper, we present theoretical studies of IR tunneling absorption in weakly tunnel-coupled n-type semiconductor double quantum wells (DQWs) (e.g., GaAs/AlGaAs) in tilted magnetic fields $\mathbf{B} = (\mathbf{B}_{\|}, \mathbf{B}_{\perp})$. The QWs are separated by a wide barrier and have a tunable energy mismatch Δ between the two ground sublevels. Inter-QW IR absorption is one of many interesting phenomena caused by tunneling between two quasi-two-dimensional (2D) electron layers [1]. Recently, Simmons proposed to use tunneling-DQW structures for tunable IR detectors [2]. In this structure, the two QWs have independent ohmic contacts [3]. In DC and AC tunneling transport and photoconductance, electrons flow in through one end of a QW, undergo resonant or photon-assisted tunneling through the barrier between the two QWs, and then flow out of the other end of the second QW. The in-plane conductances in the QWs are much larger than the tunneling conductance, yielding negligible potential drop along the current paths inside each QW. The linear driving electric field is in the direction perpendicular to the plane of the two QWs. The QWs are in equilibrium. The present study does not apply to strongly-coupled DQWs with a thin center barrier, where entirely different physical phenomena occur [1].

Our theory is valid for tunneling absorption of IR photons between the sublevels of one QW and those of the other QW. However, applications are made only to the typical situation where tunneling occurs between the two ground sublevels. The effect of spin splitting is neglected. In $\mathbf{B} = 0$, the absorption intensity decreases significantly as the line width increases with increasing temperature (T). The absorption intensity depends strongly on the electron density. In magnetic fields, the in-plane ($B_{\|}$) and perpendicular ($B_{\perp}$) components of the field are found to sensitively control and tune the absorption line shape in very different ways. The perpendicular component of the field $B_{\perp}$ tunes the cyclotron energy, relative positions of the two Landau ladders for asymmetric QWs, and the interwell spectral overlap of the density of states of the Landau levels. On the other hand, for $B_{\perp} = 0$, the in-plane field $B_{\|}$ merely shifts the relative separation of the energy-dispersion parboloids of the two QWs in k-space, tuning the absorption maxima, minimum, and the absorption edges. For $B_{\perp} > 0$, however, the in-plane field also modulates the effective tunneling strength by displacing the centroid of the initial- and final-state Landau-level wave functions.

DISCLAIMER

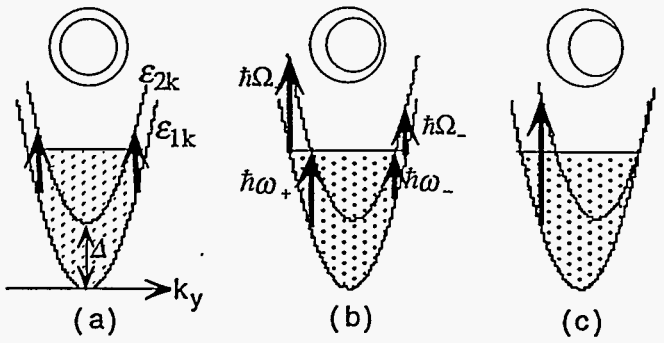

Fig.1 Relative positions of the dispersion parabolas of QW1 and QW2, with their Fermi circles, for increasing $B_{||}$ from (a) to (c). The upper parabola slides further relative to the lower one for larger $B_{||}$. The vertical arrows indicate tunneling absorptions. The arrows in (b) signify the transitions responsible for the absorption edges at $\hbar\Omega_{\pm}$ and the cusps at $\hbar\omega_{\pm}$.

TUNNELING ABSORPTION WITH IN-PLANE MAGNETIC FIELDS ($B_{\perp} = 0$)

For $\mathbf{B} = 0$ and in the effective mass (m^*) approximation, the energy-dispersion paraboloids of the two QWs are concentric, offset by Δ, as shown in Fig. 1(a) for the $k_x = 0$ plane. For nonzero Δ, DC resonant tunneling is impossible because momentum-energy conservations cannot be achieved simultaneously on the Fermi surface, owing to the fact that the two concentric Fermi circles in Fig. 1(a) do not intersect [4]. However, tunneling can occur through the absorption of photons as illustrated schematically by the vertical arrows, which originate from the occupied states of the lower parabola of QW1 and terminate at the vacant states of the upper parabola of QW2. The shaded area indicates occupied 2D electron states. The absorption lineshape is sharply peaked at the photon energy $\hbar\omega = \Delta$, yielding possible applications to IR-detector devices. The energy mismatch Δ can be tuned by applying a bias either between the two QWs or to a surface gate. As will be shown later, the absorption decreases with T due to the thermal depopulation and population of the lower and upper levels, respectively.

In $B_{||}$ applied in the x-direction, the in-plane wave vector $\mathbf{k} = (k_x, k_y)$ is still a good quantum number at low $B_{||}$ when the classical magnetic length $\ell_{||} = (\hbar c/eB_{||})^{1/2}$ is much larger than the QW widths. However, the two paraboloids are shifted in $\mathbf{k}$ space relative to each other in the k_y-direction by an amount $\Delta k_y = d/\ell_{||}^{\,2}$. This is shown for $k_x = 0$ in Fig. 1(b)- 1(c) for increasing $B_{||}$ [1]. Here d is the center-to-center distance of the QWs. Inspection of Fig. 1 implies that the absorption lineshape should change dramatically with increasing $B_{||}$, as will be shown below.

For $B_{\perp} = 0$, the absorption is given, *with or without* $B_{||}$ and to the lowest order in the zero-field tunneling integral J_o, by the real part of the tunneling conductance of the QWs:

$$G(\omega) = \frac{2\pi J_o^{\,2} e^2}{\hbar} \sum_k \int_{-\infty}^{\infty} \frac{f(z) - f(z+\hbar\omega)}{\hbar\omega} \rho_{1k}(z)\rho_{2k}(z+\hbar\omega)dz + (1 \leftrightarrow 2), \qquad (1)$$

where $f(z)$ is the Fermi function and $\rho_{ik}(z)$ is the spectral density in the i-th QW:

$$\rho_{ik}(z) = \frac{1}{\pi} \frac{\Gamma_{ik}(z)}{(z - \varepsilon_{ik})^2 + \Gamma_{ik}(z)^2}. \qquad (2)$$

The energies are given by

$$\varepsilon_{1k} = \varepsilon(k_x) + \varepsilon(k_y),$$

$$\varepsilon_{2k} = \varepsilon(k_x) + \varepsilon(k_y - \Delta k_y) + \Delta, \quad (\Delta k_y = \frac{deB_{||}}{\hbar c}) \qquad (3)$$

where $\varepsilon(q) = \hbar^2 q^2/(2m^*)$. In (2), $\Gamma_{ik}(z)$ is the imaginary part of the self-energy given in the Born approximation by $\Gamma_{1k}(z) = \Gamma_1\theta(z)$ and $\Gamma_{2k}(z) = \Gamma_2\theta(z - \Delta)$ for short-range (i.e., delta-function)

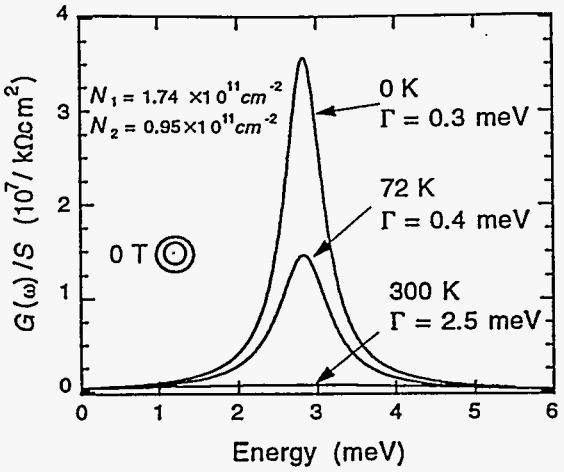

Fig. 2 The temperature dependence of G of sample 1 at $\mathbf{B} = 0$.

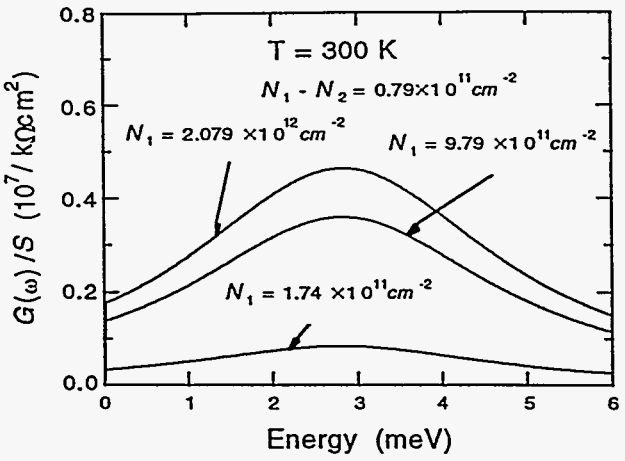

Fig. 3 The density (N_1) dependence of G of sample 1a for a fixed value of N_1 -N_2 at $\mathbf{B} = 0$.

scattering potentials. Here $\theta(z)$ is a unit step function and Γ_1 and Γ_2 are constants.

In zero magnetic field (i.e., $\mathbf{B} = 0$), $G(\omega)$ in (1) can be approximated as

$$G(\omega) = \frac{J^2 e^2 \rho_{2D}}{\hbar^2 \omega} \frac{\Gamma}{(\hbar\omega - \Delta)^2 + \Gamma^2} \left\{ \frac{1}{\beta} \ell n \frac{e^{\beta\hbar\omega} + e^{\beta(\Delta_> - \mu)}}{1 + e^{\beta(\Delta_> - \mu)}} \right\}, \tag{4}$$

where $\Gamma = \Gamma_1 + \Gamma_2$, $\beta = (k_B T)^{-1}$, $\rho_{2D} = m^* S/(\pi\hbar^2)$ is the 2D density of states, S is the area of the QWs, and $\Delta_>$ is the larger of Δ and $\hbar\omega$. Eq. (4) is exact in the limit $\Gamma_1 \to 0$ or $\Gamma_2 \to 0$. The lineshape is peaked at $\hbar\omega = \Delta$. The chemical potential μ is a function of the 2D densities of QW1 and QW2 (N_1 and N_2) and T. In Fig. 2, we show zero-field G for n-type GaAs/AlGaAs DQWs (sample 1) with $N_1 = 1.74\times10^{11}$, $N_2 = 0.95\times10^{11}$ cm^{-2}, $\Delta = 2.83$ meV, $m^* = 0.067m_0$ (m_0 is the free electron mass), $d = 21.5$ nm, and $J = 0.04$ meV [5, 6]. The $T = 0$ K value of $\Gamma = 0.3$ meV corresponds to the mobility of 57.4×10^3 cm^2/Vsec. T-dependent phonon contributions Γ_{ph} are added to $\Gamma =$ 0.3 meV for T =72 K and 300 K. Here Γ_{ph} is obtained from mobility data [7]. The absorption is broad at $T = 300$ K and weak due to an extreme depopulation of the lower level and population of the upper level in this nondegenerate gas. The intensity improves significantly for large N_1. This is seen in Fig. 3 where we show the absorption for sample 1a for increasing N_1 with a constant resonance energy Δ (i.e., constant N_1 - N_2). Sample 1a is identical to sample 1 except that it has $\Gamma =$ 2.2 meV at 300 K, corresponding to the phonon-limited mobility of 8×10^3 cm^2/Vsec.

In an in-plane magnetic field, the field-induced broadening of the absorption lineshape arising from the relative displacement of the dispersion parabolas of QW1 and QW2 is much larger than Γ in a *high-mobility* structure. In this limit (i.e., in the limit $\Gamma_1 \simeq \Gamma_2 \simeq 0$), we reduce (1) to

$$G(\omega) = \frac{J^2 e^2 S}{2\pi\hbar^2 \omega \ell d\varepsilon(\ell^{-1})} \left(F(\varepsilon^*) - F(\varepsilon^* + \hbar\omega) \right), \tag{5}$$

where $\varepsilon^* = \varepsilon(k_y^*)$, $k_y^* = [(\Delta - \hbar\omega)/\varepsilon(\ell^{-1}) + (d/\ell)^2]/2d$, and

$$F(z) = \ell \int_0^\infty \frac{dk_x}{\exp[\beta(\varepsilon(k_x) + z - \mu)] + 1}. \tag{6}$$

At $T = 0$, G in (5) can be evaluated exactly [8]. Its sensitive $B_{||}$-dependence is seen in Fig. 4 for sample 1. The $B_{||} = 0$ T lineshape is for $\Gamma = 0.3$ meV. DC tunneling is turned on at $B_{||} = 0.84$ T, where the two Fermi circles touch tangentially from inside as illustrated in the inset. The absorp-

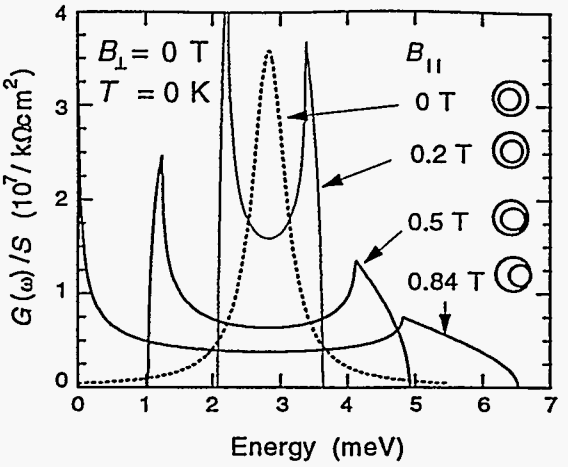

Fig. 4 The $B_{||}$-dependence of G of sample 1 with $\Gamma = 0$ meV for $B_{||} > 0$ T, and $\Gamma = 0.3$ meV for $B_{||} = 0$ T.

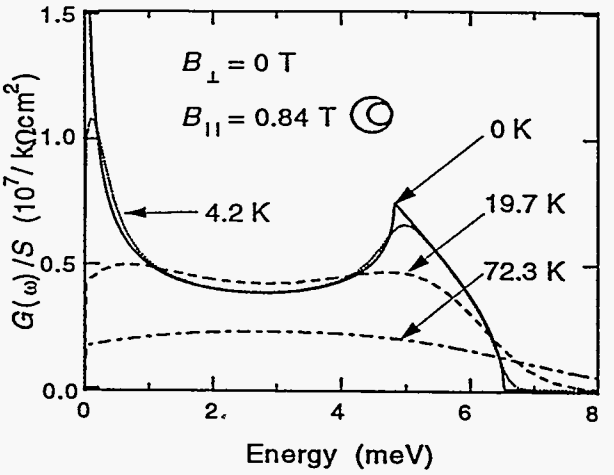

Fig. 5 The temperature dependence of G of sample 1 at $B_{||} = 0.84$ T with $\Gamma = 0$ meV.

tion diverges as $\omega^{-1/2}$ for $\omega \to 0$. $B_{||}$-dependent behavior of the DC tunneling conductance has been studied earlier in detail and will not be discussed here [4 - 6, 9]. The deep minimum in the $B_{||}$ - dependent absorption, with sharp cusps at both edges, arises from the forbidden absorption into the Fermi sea of QW2. The sharp cusps and absorption edges are rounded for $\Gamma > 0$. The absorption minimum is absent for sample 2 in Fig. 6. The parameters of sample 2 are the same as those of sample 1 except that QW2 is empty (i.e., $N_2 = 0$) and $\Delta = 6.7$ meV. The physical origin for the absorption edges ($\hbar\Omega_\pm$) and the cusps ($\hbar\omega_\pm$) in Fig. 4 are illustrated in Fig. 1. The sharp edges of G are rounded at finite T as shown in Fig. 5 at $B_{||} = 0.84$ T for sample 1.

TUNNELING ABSORPTION IN TILTED MAGNETIC FIELDS ($B_\perp > 0$)

When a perpendicular component $\mathbf{B}_\perp$ // **z** is added to an in-plane field $\mathbf{B}_{||}$, Landau levels are formed and the plane wave picture above is no longer valid. The interwell tunneling integral

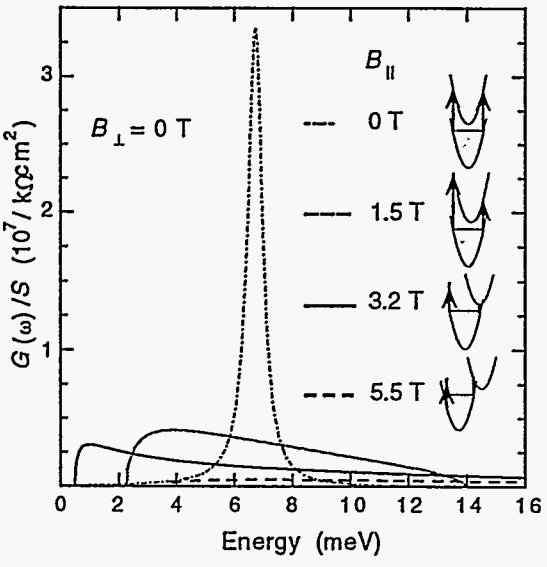

Fig. 6 Absorption per area of sample 2 with $N_2 = 0$, $\Gamma = 0.3$ meV for $B_{||} = 0$ T, and $\Gamma = 0$ meV for $B_{||} > 0$ T.

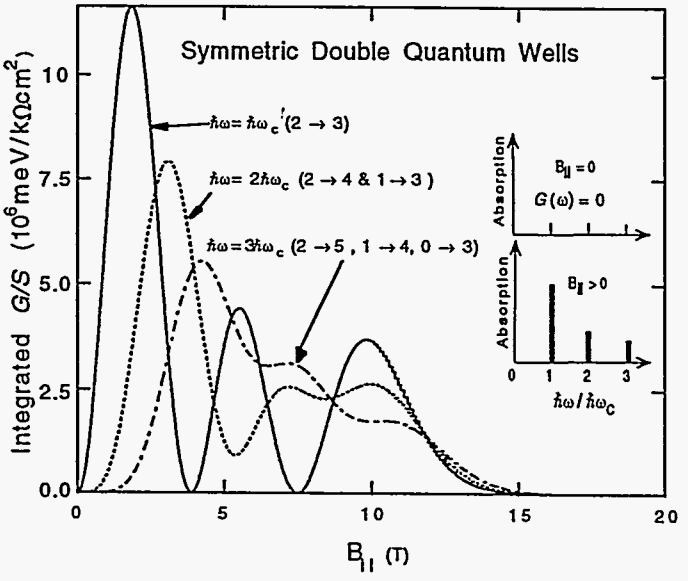

Fig. 7 Integrated absorption per area of sample 3 for $B_\perp = 2.8$ T. The inset illustrates the absorption spectra.

between Landau levels n and n' is given by [10]

$$J_{n,n'} = (-1)^{n_>-n_<} J_o e^{-x/2} (n_<!/n_>!)^{1/2} x^{(n_>-n_<)/2} L_{n_<}^{n_>-n_<}(x), \tag{7}$$

where $n_>$ ($n_<$) is the larger (lesser) of (n, n'). $L_n^m(x)$ is the associated Laguerre polynomial and $x = \alpha^2/2 = (d/\ell_{||})^2 B_{||}/2B_\perp$. Note that $J_{n,n'} = J_0 \delta_{n,n'}$ for $B_{||} = x = 0$, namely, only the $n \rightarrow n' = n$ interwell transitions are allowed in the absence of $B_{||}$.

The absorption is given by

$$G = \frac{2\pi e^2 g}{\hbar} \sum_{n,n'} J_{n,n'}^2 \int_{-\infty}^{\infty} \frac{f(z) - f(z+\hbar\omega)}{\hbar\omega} \rho_{1n}(z) \rho_{2n'}(z+\hbar\omega) dz + (1 \leftrightarrow 2), \tag{8}$$

where $g = S/(2\pi\ell_\perp^2)$ is the Landau level degeneracy per spin, $\ell_\perp = (\hbar c/e B_\perp)^{1/2}$ and

$$\rho_{in}(z) = \frac{1}{\pi} \frac{\Gamma_{in}(z)}{(z-\varepsilon_{in})^2 + \Gamma_{in}(z)^2}. \tag{9}$$

Here $\Gamma_{in}(z)$ is the imaginary part of the self-energy for the Landau level energies given by

$$\varepsilon_{1n} = (\frac{1}{2} + n)\hbar\omega_c, \quad \varepsilon_{2n'} = (\frac{1}{2} + n')\hbar\omega_c + \Delta, \tag{10}$$

where $\omega_c = eB_\perp/m^*c$. Eqs. (8) - (10) can be reduced to Eqs. (1) - (3) by using asymptotic expressions for $L_n^m(x)$ in the limit $B_\perp \rightarrow 0$ (i.e., $x \rightarrow \infty$) [11].

According to (7), tunneling can occur only between the Landau levels with same quantum numbers n in the absence of $B_{||}$. With nonvanishing $B_{||}$, the intensities of $n \rightarrow n$ transitions diminish while those of $n \rightarrow n'$ ($\neq n$) transitions grow from zero initially and then oscillate with increasing $B_{||}$. This is illustrated in Fig. 7 for symmetric DQWs (sample 3) for $\Gamma \rightarrow 0$. Here, resonant photon energies are given by $\hbar\omega = \delta n \hbar\omega_c$ where $\delta n = n' - n = 1, 2, \cdots$. The parameters of sample 3 are given by $N_1 = N_2 = 4\times10^{11}$ cm^{-2}, $J_0 = 0.04$ meV, and $d = 17.5$ nm. Three Landau levels are filled at $B_\perp = 2.8$ T, where $\hbar\omega_c = 4.9$ meV. Resonant DC (i.e., $n \rightarrow n$) tunneling is negligible because the Fermi level is halfway between the Landau levels $n = 2$ and $n = 3$, where the density of states is zero. The intensities for the $\hbar\omega = 2\hbar\omega_c$ and $\hbar\omega = 3\hbar\omega_c$ absorption arise from the superpositions of two and three transitions respectively as indicated in Fig. 7. As a result, their minima do not become zero.

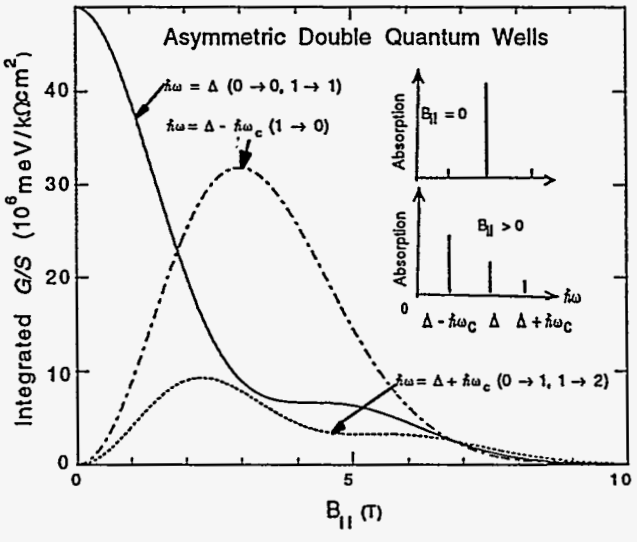

Fig.8 Integrated absorption per area of sample 4 for $B_\perp = 2.1$ T with $N_2 = 0$. The inset illustrates the absorption spectra.

In Fig. 8, we plot the integrated absorption from sample 4 where only QW1 has carriers. For sample 4, $N_1 = 2\times10^{11}$ cm^{-2}, $N_2 = 0$, $\Delta = 5.0$ meV, $J_0 = 0.04$ meV, and $d = 17.5$ nm at $B_\perp$

= 2.1 T, where $\hbar\omega_c = 3.6$ meV and two Landau levels $n = 0, 1$ of QW1 are filled. Note, however, that some electrons migrate back to QW2 from QW1 (i.e., $N_2 > 0$) at $B_\perp = 0$ since the Fermi energy (at $B_\perp = 0$ T) is larger than Δ. In this sample, transitions $0 \rightarrow \delta n$ ($\delta n = 0, 1, \cdots$) and $1 \rightarrow 1 + \delta n$ ($\delta n = -1, 0, 1, \cdots$) from QW1 to the empty levels of QW2 yield resonant absorption of photons of energy $\hbar\omega = \delta n\hbar\omega_c + \Delta$ as shown in Fig.8. The intensity for the $\hbar\omega = \Delta$ transition drops with increasing $B_\parallel$, while that of $\hbar\omega = \delta n\hbar\omega_c + \Delta$ ($\delta n \neq 0$) transition grows from zero and oscillate.

CONCLUSIONS

We have employed a linear-response theory to study the interwell-tunneling absorption in tilted magnetic fields in weakly-coupled n-type symmetric and asymmetric double QWs with a tunable energy mismatch between the two ground sublevels. Photon-assisted tunneling occurs between the ground sublevels of the QWs. We have shown that applied magnetic fields sensitively alter the threshold energy, the resonance energy, and the linewidth. In zero magnetic field, the absorption intensity decreases significantly as the linewidth increases with the temperature. The absorption intensity depends strongly on the electron density. In magnetic fields, both the in-plane and perpendicular components of the field are found to sensitively control and tune the absorption line shape in very different ways. The perpendicular component of the field tunes the cyclotron energy, relative positions of the two Landau ladders for asymmetric QWs, and the interwell spectral overlap of the density of states of the Landau levels. In the absence of a perpendicular component of the field, the in-plane field merely shifts the relative separation of the energy-dispersion parboloids of the two QWs in k-space, tuning the absorption maxima, minimum, and the absorption edges. In the presence of a finite perpendicular component of the field, however, the in-plane field also modulates the effective tunneling strength by displacing the centroid of the two Landau-level wave functions involved in the transition.

ACKNOWLEDGMENTS

The author wishes to thank Dr. J. A. Simmons for a careful reading of the manuscript and helpful comments. This work was supported by U.S. DOE under Contract No.DE-AC04-94AL85000.

REFERENCES

1. See S. K. Lyo, J. A. Simmons, N. E. Harff, T. M. Eiles, and J. F. Klem, Inst. Phys. Conf. Ser. No 145, p 845 (IOP Publishing Ltd, 1996) and references therein.
2. J. A. Simmons, unpublished.
3. J. P. Eisenstein, L. N. Pfeiffer, and K. W. West, Appl. Phys. Lett. **57**, 2324 (1990).
4. J. P. Eisenstein, T. J. Gramila, L. N. Pfeiffer, and K. W. West Phys. Rev. B **44**, 6511 (1991).
5. S. K. Lyo and J. A. Simmons J. Phys.: Condens. Matter **5**, L299 (1993).
6. J. A. Simmons, S. K. Lyo, J. F. Klem, M. E. Sherwin, and J. R. Wendt Phys. Rev. B **47**, 15741(1993).
7. J. H. English, A. C. Gossard, H. L. Stormer, and K. W. Baldwin, Appl. Phys. Lett. **50**, 1826 (1987).
8. S. K. Lyo, Superlattices and Microstructures, Vol. 20, No. 3 (1996), in press.
9. L. Zheng and A. H. MacDonald Phys. Rev. B **47**, 10619(1993).
10. J. Hu and A. H. MacDonald, Phys. Rev. B **46**, 12554 (1992).
11. S. K. Lyo (unpublished).